Journal of Power Sources 331 (2016) 224–231

Contents lists available at ScienceDirect

Journal of Power Sources

journal homepage: www.elsevier.com/locate/jpowsour

Extending battery life: A low-cost practical diagnostic technique for lithium-ion batteries

Yu Merla [a, *], Billy Wu [b], Vladimir Yufit [c], Nigel P. Brandon [c], Ricardo F. Martinez-Botas [a], Gregory J. Offer [a, c]

[a] Department of Mechanical Engineering, Imperial College London, Exhibition Road, South Kensington Campus, London, SW7 2AZ, UK
[b] Dyson School of Design Engineering, Imperial College London, Exhibition Road, South Kensington Campus, London, SW7 2AZ, UK
[c] Department of Earth Science and Engineering, Imperial College London, Exhibition Road, South Kensington Campus, London, SW7 2AZ, UK

HIGHLIGHTS

- Differential Thermal Voltammetry (DTV) carried out on battery packs under cooling.
- Technique can cope with unknown, unequal and changing current between cells.
- DTV diagnosed the state of health of individual cells under charge/discharge.
- Easy installation to existing systems due to simple hardware/software requirements.
- Differential heat flux voltammetry introduced as a complimentary method.

ARTICLE INFO

Article history:
Received 15 June 2016
Received in revised form
18 August 2016
Accepted 3 September 2016

Keywords:
Lithium-ion battery
Battery pack
Degradation
State-of-health
Differential thermal voltammetry
Differential heat flux voltammetry

ABSTRACT

Modern applications of lithium-ion batteries such as smartphones, hybrid & electric vehicles and grid scale electricity storage demand long lifetime and high performance which typically makes them the limiting factor in a system. Understanding the state-of-health during operation is important in order to optimise for long term durability and performance. However, this requires accurate in-operando diagnostic techniques that are cost effective and practical. We present a novel diagnosis method based upon differential thermal voltammetry demonstrated on a battery pack made from commercial lithium-ion cells where one cell was deliberately aged prior to experiment. The cells were in parallel whilst being thermally managed with forced air convection. We show for the first time, a diagnosis method capable of quantitatively determining the state-of-health of four cells simultaneously by only using temperature and voltage readings for both charge and discharge. Measurements are achieved using low-cost thermocouples and a single voltage measurement at a frequency of 1 Hz, demonstrating the feasibility of implementing this approach on real world battery management systems. The technique could be particularly useful under charge when constant current or constant power is common, this therefore should be of significant interest to all lithium-ion battery users.

1. Introduction

In order for hybrid & electric vehicles to compete with internal combustion engine vehicles, they must meet the high power and energy requirements demanded from modern applications at an acceptable cost [1]. A major factor slowing down the transition to electric vehicles is the cost of the battery pack [2] which for example in Tesla vehicles account for approximately one quarter of the total production cost [3].

Understanding battery lifetime is essential in order to maximise the economics of batteries; if a battery reaches its end-of-life (EOL) before the EOL of the product then it must be replaced, incurring significant cost for either the consumer or the OEM under warranty, and this can also affect the residual value for second life applications. Battery lifetime is a function of degradation, which involves multiple coupled & path dependent degradation mechanisms, yet,

* Corresponding author.
E-mail addresses: yu.merla09@imperial.ac.uk (Y. Merla), billy.wu@imperial.ac.uk (B. Wu), v.yufit@imperial.ac.uk (V. Yufit), n.brandon@imperial.ac.uk (N.P. Brandon), r.botas@imperial.ac.uk (R.F. Martinez-Botas), gregory.offer@imperial.ac.uk (G.J. Offer).

http://dx.doi.org/10.1016/j.jpowsour.2016.09.008
0378-7753/

industry standard measures of degradation or state-of-health (SOH) are based upon simple capacity and power fade. Capacity fade is defined as the percentage decrease of capacity compared to beginning of life (BOL) typically carried out under 1C discharge at 25 °C. Power fade can be defined as the percentage increase in the real impedance measured at 1 kHz but often at an unspecified state-of-charge (SOC).

Batteries degrade through various mechanisms over time [4,5] and individual cells in a pack may age differently [6]. Unfortunately, it is possible for 2 cells that have been used differently to have the same degree of capacity fade, and even power fade, yet for one of them to be safe to use for many more cycles and the other not. Hence these crude measures of degradation are wholly unsuitable for most applications. This is even possible within a single battery pack, due to thermal inhomogeneities within a pack and/or unequal current paths between cells in parallel or within large cells [6]. This unequal degradation can lead to reduced overall pack performance and lifetime which means particular cells may need to be controlled or replaced accordingly. Hence a good and low-cost diagnosis method capable of accurately identifying such cells with detailed state-of-health information is required.

Considerable research has been carried out to develop new techniques to monitor battery SOH however many are not suitable for in-operando use as they require expensive equipment such as electrochemical impedance spectroscopy (EIS) [7,8], in-situ nuclear magnetic resonance [9] or X-ray computational tomography [10,11]. Data mining techniques such as extended Kalman filters [12], neural network and linear prediction error methods [13] have also been researched for SOH estimation in a BMS. Many in-operando techniques based on the temperature measurements are mostly derived from the original work by Maher and Yazami [14] who made entropy and enthalpy measurements at specific cell potentials giving information on the state of both electrodes. The techniques using current are usually called incremental capacity analysis, and are exemplified by the latest work of DuBarry et al. [15] who have developed models which compare the dQ/dV peaks with its fresh cell equivalent to quantify cell SOH in terms of degradation modes such as loss of lithium inventory, loss of active materials and ohmic resistance increase. In their work, each dQ/dV spectra represents a combination of processes at both positive and negative electrodes. However, little work has been done on how to implement these techniques at a pack level although Offer et al. has demonstrated a relatively simple method to identify a faulty cell and/or connection in a battery pack [6] by measuring the potential drop of each cell during a current interrupt tests.

The method of Differential thermal voltammetry (DTV) [16,17] was previously reported by the authors as a complimentary tool to incremental capacity analysis (ICA), showing how simple temperature measurements could be used to infer similar information. DTV only requires temperature and voltage measurements and is carried out by measuring the change in cell surface temperature during constant current discharge and does not require temperature to be carefully controlled. The DTV parameter, dT/dV is calculated by taking the time differential of the temperature, dT/dt divided by the time differential of the potential, dV/dt. Plotted against cell potential, the result gives similar information as ICA and slow rate cyclic voltammetry but with additional data about the entropic state of the electrodes.

DTV was presented as a suitable diagnosis method for use in real-world applications, however the previous validation experiments were all carried out on individual cells under natural convection thermal boundary conditions. In high power applications such as in electric vehicles, the cells would be connected in a pack with a thermal management system to maintain the cells at safe operating temperature. In addition, the experiment was only validated for constant current discharge which meant that the diagnosis required a dedicated discharge cycle, which is uncommon in many applications.

In this paper, DTV experiments have been carried out on a battery pack made from four commercial lithium polymer cells in parallel placed under forced air surface cooling to emulate an electric vehicle application. One cell was deliberately aged prior to the experiments to demonstrate how the technique could diagnose unequal degradation. The test was performed at both constant current charge and discharge to demonstrate its use under charging conditions. Differential heat flux voltammetry (DHFV), dHF/dV is also introduced as a complementary method when dT/dt is too small to measure accurately under strong cooling conditions.

2. Methods

2.1. Battery testing

The experiment was performed using a battery pack made from four commercial 5 A h lithium-polymer pouch cells connected in parallel (Dow Kokam, model SLPB11543140H5) where each cell consists of a carbon graphite negative electrode and a nickel-manganese-cobalt ($Ni_xMn_yCo_z$) positive electrode. Heat flux sensors with K-type thermocouples (OMEGA HFS-4) were placed on the surface at the centre of the cell. Shunt resistors (RS 810-3273) were placed in series with each cell to measure the current across every individual cell. It should be noted, that current measurements were undertaken in order to compare the DTV technique to ICA and to understand how the current changes for cells in parallel, but the current measurement is not required for, and was not used for the DTV calculation. One deliberately aged cell and three fresh cells were placed together in the pack to determine whether the diagnosis methods could correctly determine the SOH of the individual cells. The aged cell was previously stored at 55 °C at 4.2 V for approximately 15 days. The pack was prepared in a way to minimise differences in external resistance such as equal cable lengths, fastening torque (8 kNm) and cleaned contact surfaces.

During the experiments, the pack was placed inside an incubator (Binder KB-23) with forced air convection flowing over the pack surface (as illustrated in Fig. 1) while keeping the incubator door open to emulate a surface cooling system to recreate real conditions such as those in electric vehicles. A Maccor Battery Tester series 4000 was used for measurements and loading during pack experiments whereas a Bio-Logic BCS-815 was used for individual cell experiments. Pico TC-08 was used for heat flux sensor

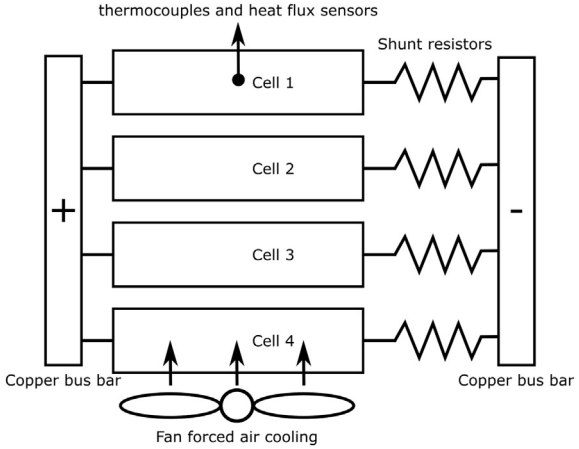

Fig. 1. Experimental set-up for pack analysis.

measurements and Yokogawa MX100 for shunt resistor measurements.

The pack experiment was carried out at 2C constant current charge and discharge to diagnose the individual cells simultaneously in the pack using DTV, DHFV and ICA. The same experiment was repeated for 0.5C to demonstrate the use of the technique under both fast and slow charging/discharging conditions. The 0.5C results are attached as supplementary material effectively demonstrating the same results as 2C. Then the cells were individually characterised through constant current discharges at 1/3C, 1C and 2C to determine their SOH through capacity fade. Detailed condition of test is described in Table 1.

2.2. Data processing

Depending on the noise of data acquisition, it is necessary to smooth the raw data before evaluation. In this experiment, a moving average was used to smooth the temperature or heat flux data. Due to the accuracy of the sensors used, the heat flux measurements were particularly noisy. Care must be taken during smoothing as to not lose the characteristic of the curve through over-smoothing. In order to make sure of this, the median of the absolute residuals was kept below 0.1% for temperature and 7.5% for heat flux. In addition, changing smoothing parameters such as the span can have an effect on peak fitting. For this reason, the smoothing conditions were kept identical for the 4 cells for a particular loading (charge or discharge) and diagnosis (DTV or DHFV). Peak fitting errors were kept to a maximum of 3.3%.

3. Results

Fig. 2 shows pack experimental results for 2C (40 A) discharge. In an ideal battery pack, each cell is expected to provide 10 A. However, Fig. 2a shows that the current paths between the four cells are heterogeneous. The three fresh cells have relatively similar current profile whereas the aged cell performs very differently. This is also reflected in the dQ/dV plot of Fig. 2b as the different current profile results in different dQ term. This is due to the changes in overpotential and electrode stoichiometries for the aged cell. Overpotential is defined as the drop in potential due to internal resistances such as ohmic, ionic, charge transfer and diffusion.

It is observed that the three fresh cells initially discharge at slightly higher than 10 A to compensate for the low power performance of the aged cell. However, towards the end of its loading, the aged cell experiences higher current for the given pack voltage where it peaks at 2.86C (14.3 A). This may be as result of 3 cells having increased impedance due to the deep discharge while the aged cell still has not gotten to that stage and has slightly lower impedance thus delivering higher current. Operating at higher current accelerates degradation mechanisms such as lithium plating on charge and electrolyte decomposition by higher heat generation [4,5]. Hence it is crucial for a battery management system to be able to correctly identify unhealthy cells to be replaced at an early stage.

Fig. 2a also shows internal current during relaxation. At the end of discharge, the cells were at different OCVs and therefore after removal of load the aged cell recharges the good cells for an appreciable length of time. This further loads the cells and over time can get worse and could lead to additional degradation. It was shown in previous work that for a noisy load, this redistribution effect can be continuous and significant, leading to the net current throughput through the cells being significantly higher than otherwise [18], which again could lead to additional degradation.

Fig. 2c and d shows DTV and DHFV results respectively. The notable differences can be immediately observed between the aged cell and the fresh cells.

The peak in the dT/dV, or the plateau in the voltage curve, represents a combination of different contributions from the positive and the negative electrode phase. It corresponds to a region where an electrode phase is not changing, but the concentration of lithium in that phase is increasing or decreasing [20,21]. Then, at some critical concentration the lattice structure of the material becomes unstable, and the material undergoes a phase change to a new lattice structure which is more stable at the given concentration of lithium. At this point the voltage shifts dramatically, and hence the phase change is associated with moving from one peak to another.

Peak fitting analysis of the results were carried out using peakfit.m script [22] in MATLAB where the differences in the peak parameters such as the peak position and width can give information on the cell's state-of-health [17,23]. Fig. 3a and b demonstrates example peak fittings of DTV curves where each peak has been labelled accordingly for a combination of nickel-manganese-cobalt electrode phase (①-②) [24–26] and a graphitic carbon phase (❶-❻) [27]. The schematic above the plot illustrates this concept of combined electrode phases corresponding to regions of voltage plateaus, and hence peaks in the dT/dV measurement.

It can be seen in Fig. 3c and d that the aged cell has a lower ①*❶ peak potential and a wider peak width than the fresh cells for both DTV and DHFV. Peak width is taken as the width of the peak at its half height. As illustrated above Fig. 3a, degradation in the cell can result in stoichiometric drift which will change the peak parameters such as position and width. Using this method, it is possible to quantitatively diagnose the cell SOH and determine that cell 1 has significantly aged compared to the remaining fresh cells.

It can also be confirmed from this diagnosis that, if necessary, it is sufficient to analyse only peak ①*❶, which is the first peak during discharge at approximately 3.9 V. In Fig. 3a and b, it is observed that there is minimal overlap of the peaks above 3.8 V. This suggests that DTV does not need to be carried out through the entire potential range of the cell which will further reduce the time of diagnosis i.e. it may be sufficient to discharge from 4.2 V to 3.8 V to identify the aged cell.

In practice if the peak position of a particular cell is significantly shifted to a lower potential and/or the peak width is wider than the rest of the cells in a pack, it can be assumed that the pack has unequal current distribution.

In many real applications, such as in electric vehicles, it would be much more practical to be able to conduct the diagnosis under a constant current charge. This would enable the diagnosis to be carried out when the electric vehicle is left to charge and no dedicated charging or discharging profile is required.

Table 1
Experiment details.

	Loading condition	Cut-off voltage	Initial condition
Pack discharge	2C constant current	2.7 V	CCCV charging at 1C to 4.2 V until I < 0.25 A followed by 1 h rest
Pack charge	2C constant current	4.2 V	CCCV discharging at 1C to 2.7 V until I > −0.25 A followed by 1 h rest
Cell discharges	1/3C, 1C and 2C constant current	2.7 V	CCCV charging at 1C to 4.2 V until I < 0.1 A followed by 1 h rest

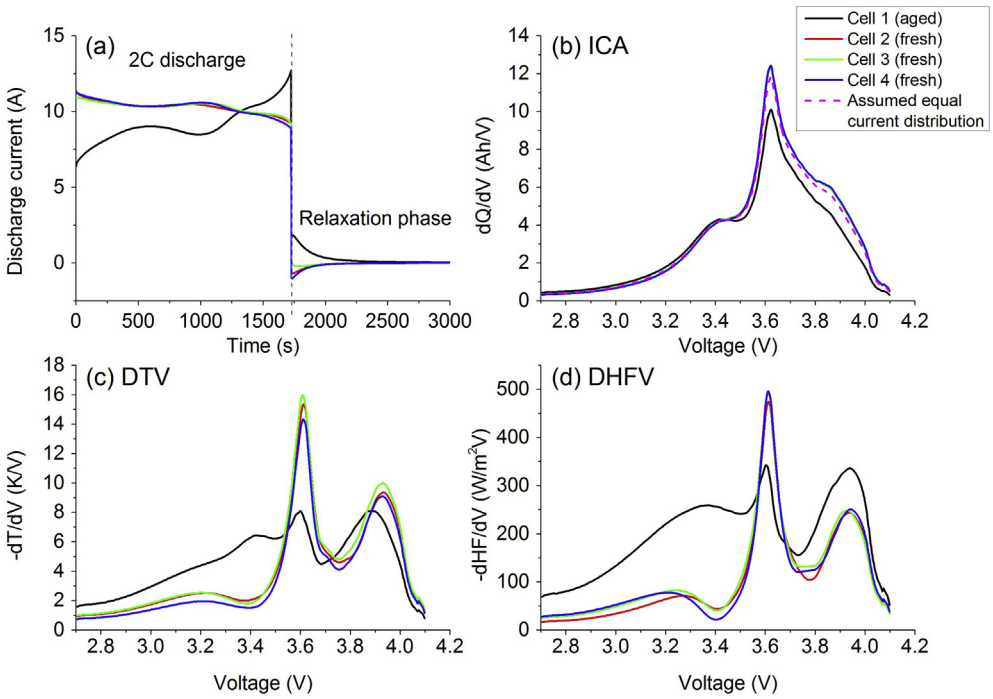

Fig. 2. Pack analysis under 2C constant current discharge. (a) Cell current. (b) Incremental capacity method. (c) Differential thermal voltammetry. (d) Differential heat flux voltammetry.

Fig. 4 shows results for a 2C (40 A) charge, typical charging rates for a fast charge for an electric vehicle. The resulting curves look different from discharge results due to the differences in power performance and entropic heat generation. However, the aged cell can still be identified for both DTV and DHFV. The negative peak in Fig. 4c and d appears from the negative dT/dt when the heat transfer from cooling dominates over the enthalpic and entropic heat generation, and where the entropic heat generation term likely became close to zero or even negative.

Fig. 5a shows the DTV result during 2C charge with a zoomed in figure on the negative peak. The negative peak here represents peak ①*❷ which is negative due to the negative dT/dt term. The notable and interesting difference with the DTV analysis during charge is the presence of two $dT/dV = 0$ transitions. dT/dV approaches zero as dV/dt is significantly higher than dT/dt i.e. a significant change in voltage while temperature remains almost unchanged. As mentioned before the phase transition is associated with a considerable change in voltage therefore as the crystallographic structure changes, the cell potential at $dT/dV = 0$, or a minima between two peaks, can be used as a footprint to track phase transition points hence electrode stoichiometry.

Fig. 5b, c and d demonstrate the potential at the initial x-axis intersect (i.e. $dT/dV = 0$ and $dHF/dV = 0$), the potential at the lowest point of the peak and second x-axis intersect respectively. It can be seen from all three parameters that the aged cell has a notably higher potential than the fresh cells for both DTV and DHFV because of a combination of increase in resistance and stoichiometric shift in the electrodes. When the phase transition occurs at $dT/dV = 0$, it is particularly useful for tracking the degradation as it requires less computations and peak fitting is unnecessary. In practice, it is recommended to use the potential at the initial x-axis intersect as the change is larger and hence is less sensitive to the inaccuracies in the voltage measurements. Here the use of DTV and DHFV has been demonstrated for an on-board identification of aged cells in a battery pack under thermal management system during charge.

The pack was then dismantled and characterisation tests were carried out on the individual cells to prove the correct cell had been identified. The experimental setup was exactly the same but the cells were loaded individually. Constant current discharges at 1/3C, 1C and 2C were performed, and their capacity is shown in Table 2. The results clearly show that cell 1 was the aged cell with 91% of its initial capacity at 2C discharge, in agreement with the DTV and DHFV diagnosis.

4. Discussion

Existing BMS are typically very simple, and have been designed to meet minimum specifications for safety and monitoring, to prevent over-heating and over charging/discharging. The measurements they take are then typically compared to empirically validated equivalent circuit models in order to estimate SOC or state-of-power (SOP). SOH prediction is typically based upon energy throughput models or simple recalibration of the capacity after a complete charge or discharge [20,28,29]. As mentioned above, it is possible for cells that have been aged in different ways to have the same capacity fade, and even power fade, and standard techniques are not capable of diagnosing the differences. In addition, if cells are in parallel with each other, unless the individual currents are measured, it is not currently possible to identify differences in SOH between the cells quickly and easily. Other more advanced techniques such as EIS require additional hardware to be implemented which comes at a cost. EIS is also highly sensitive to temperature, which although making them useful for internal temperature estimation, makes them impractical for SOH diagnosis in most cases [30–32]. ICA is probably the most useful of the existing techniques, although it requires accurate current measurement for each cell, which can be impractical for cells in parallel. Again, this technique is sensitive to temperature affecting the peak positions due to the exponential relationship between impedance

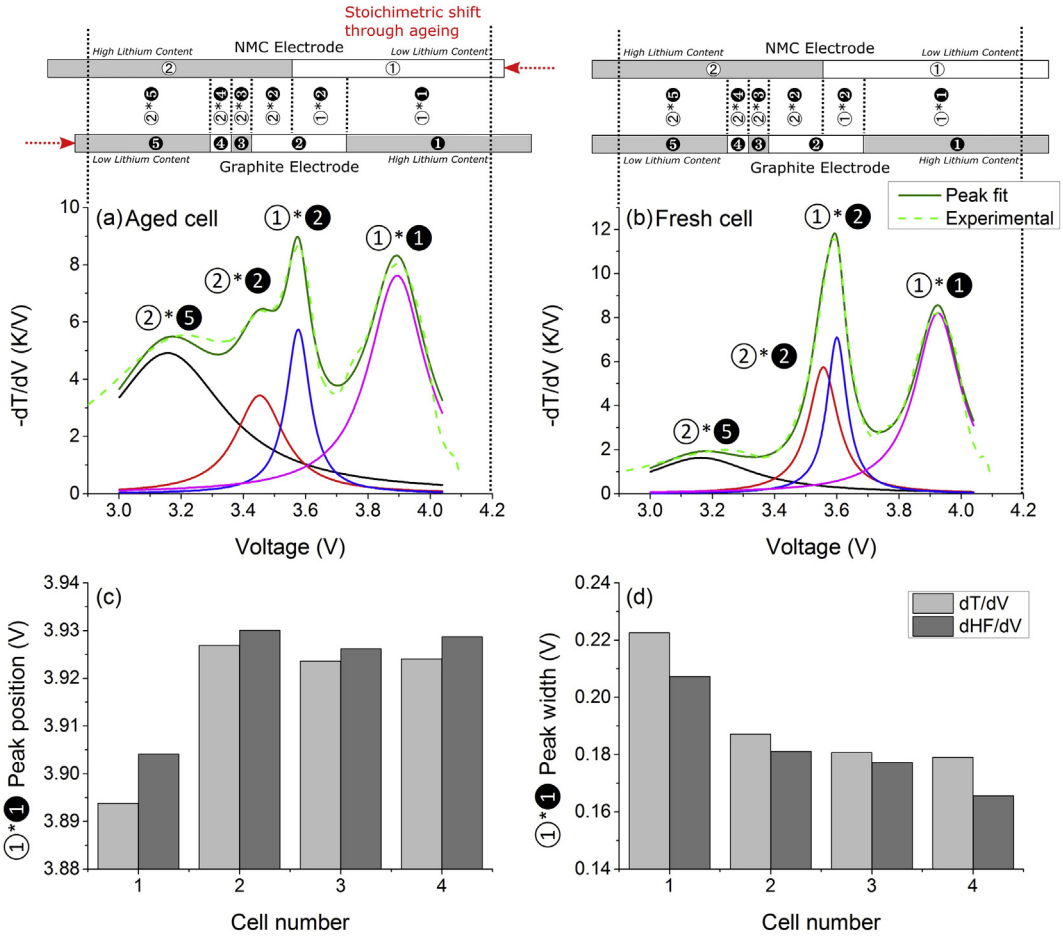

Fig. 3. Peak fitting of differential thermal and heat flux voltammetry results for 2C constant current discharge. Example peak fittings for cell 1 (a) and cell 4 (b). Schematics of combined phases in graphitic carbon negative electrode and NMC positive electrode are shown above. Schematic modified from Ref. [19] with different positive electrode chemistry and addition of effect of stoichiometric drift through ageing. Peak position (c) and peak width (d) are shown here.

and temperature. There is therefore a need for a more sophisticated technique that can be used to diagnose the SOH of individual cells even when they are in parallel and in a noisy temperature changing environment. In order to be used in real world applications a diagnostic technique must also be low cost which means it must use a limited number of cheap sensors and require minimal computational power and memory monitored at low frequencies.

It is accepted that pack design can give rise to inhomogeneity in both current and temperature between cells [18]. The unequal and changing current in the cells as observed in Figs. 2a and 4a is a result of differences in internal impedance and external resistance. The difference in internal impedance will depend on the cell's SOH, SOC, temperature and manufacturing inequalities [31,32]. The difference in external resistance arises from different contact resistances, wire length and cell's proximity to the loading point on the copper bus bar [6]. The unequal temperature is then caused by the differences in internal current, impedance and thermal boundary conditions. This can lead to both negative and positive feedback during operation. For a diagnosis technique to be suitable for implementation in a pack application, it must also be insensitive to these effects.

In this work the slight differences observed between the three fresh cells are likely to be a combination of manufacturing inequalities, differences in contact resistances and thermal boundary condition. As illustrated in Fig. 1, cell 4 is closest to the cooling fan than cell 3 followed by cell 2 and cell 1. However, the differences in performance between cells 4, 3 and 2, are minimal and confirm that almost equal cooling for all cells was achieved. In the same way the external resistances were balanced so they were insignificant compared to the differences between the cell impedances. For optimal thermal diagnosis it is ideal to have homogeneous thermal boundary conditions i.e. equal cooling for all cells in a pack.

In real application such as in electric vehicles where there are many more cells to be measured, the diagnosis may be challenging in the presence of noise and small inconsistencies between healthy cells as discussed above. In such cases data mining techniques can be used to evaluate changes from healthy to faulty cells in order to maintain diagnosis performance on a BMS [33].

Despite the changing currents between the cells, and active cooling, the aged cell was correctly identified and meaningful information was obtained as seen in both Figs. 3 and 5. The results are comparable to the single cell test under natural convection carried out in our previous work [17]. This work also demonstrates the use of the technique under charge for the first time, and the use of heat flux measurement instead of temperature. However, the heat flux sensors required for DHFV cost significantly more than regular thermocouples required for DTV. Therefore, the use of DHFV is only suggested when accurate dT/dt is difficult to measure in applications with high cooling requirements.

Due to the simple requirements of measurements and computation, this method can be applied to various real systems such as smartphones, laptops, electric vehicles and grid level storage, all at

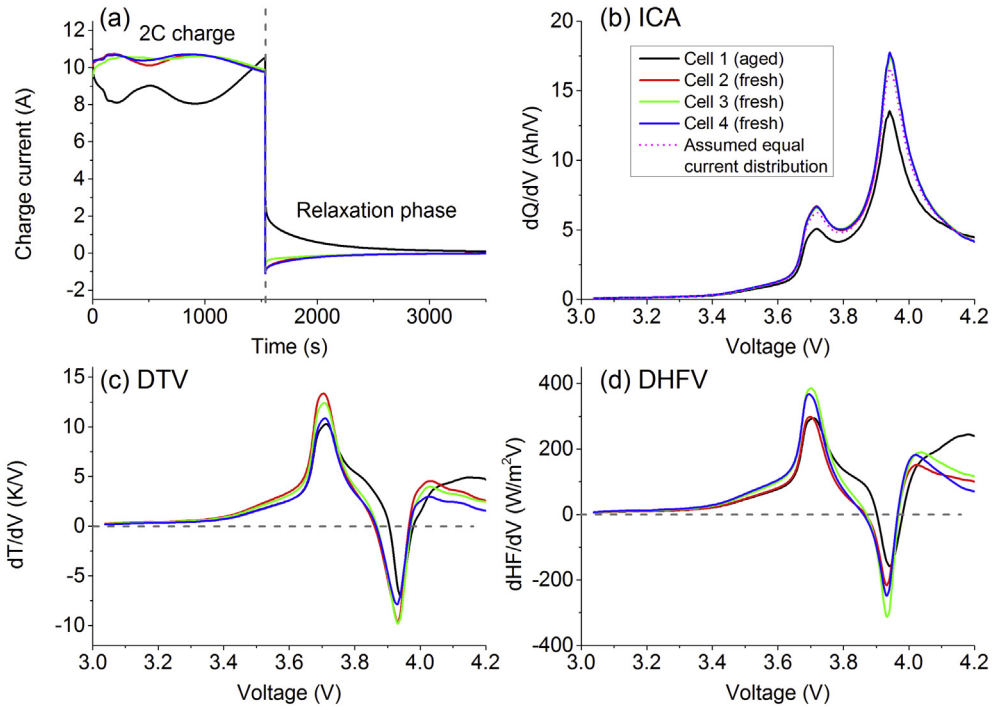

Fig. 4. Pack analysis under 2C constant current charge. (a) Cell current. (b) Incremental capacity method. (c) Differential thermal voltammetry. (d) Differential heat flux voltammetry.

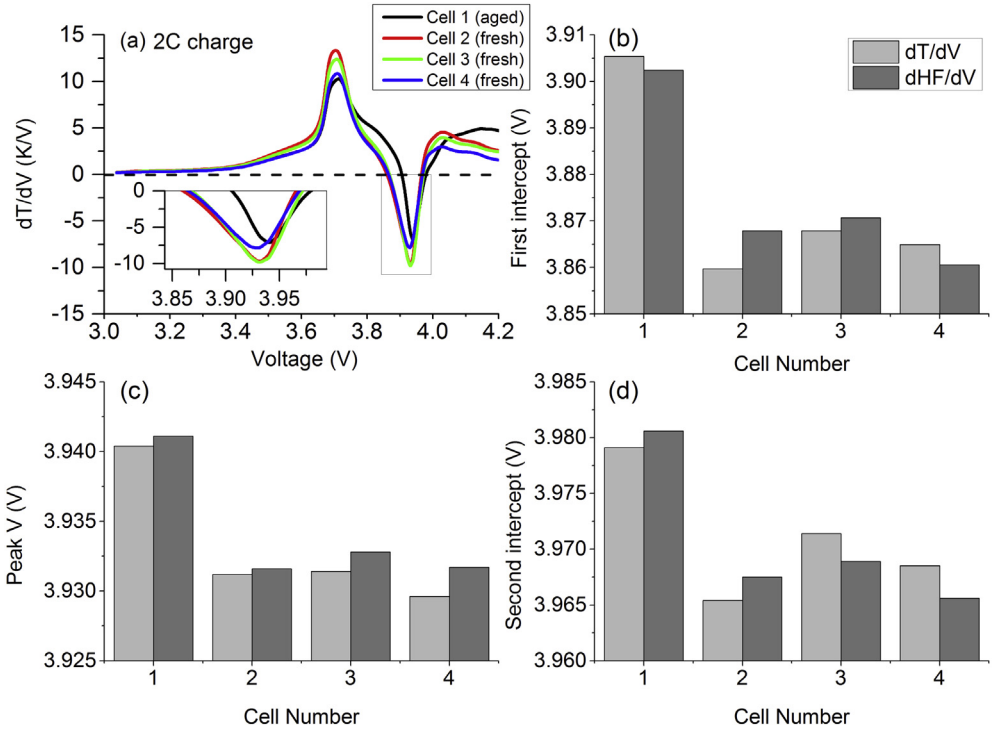

Fig. 5. Peak analysis of differential thermal and heat flux voltammetry results for 2C constant current charge. (a) Zoomed in differential thermal voltammetry result. First 0-intersect potential (b), peak potential (c) and second 0-intersect potential (d) for the negative peak are shown here.

a low cost. The importance of its application is to monitor the detailed SOH of the battery system and then to adapt its operating conditions for the given diagnosis to maximise its lifetime and prevent catastrophic failure. This is especially required for pack applications where the whole system is limited by its weakest cell.

5. Conclusion

In this paper, novel thermal diagnosis methods were performed on a pack of commercially available lithium-ion batteries. Four cells were placed in parallel where one of them was deliberately aged

Table 2
Discharge capacity of individual cells at various C-rates.

	Discharge capacity (Ah)		
	1/3C	1C	2C
Cell 1	4.65	4.53	4.39
Cell 2	5.05	4.97	4.83
Cell 3	5.06	4.97	4.83
Cell 4	5.05	4.97	4.82
Total	19.81	19.44	18.87

prior to the experiment. The pack was placed under forced air cooling to emulate a thermal management system in a real-world application and tested under a 2C charge and discharge.

Differential thermal voltammetry and differential heat flux voltammetry both correctly identified the aged cell within the pack for both charge and discharge with unknown, changing and different currents between the cells. The methods quantitatively measured an advanced state-of-health parameter through diagnosing stoichiometric shift between the two electrodes. DHFV was demonstrated to provide a complimentary diagnosis method using heat flux instead of temperature during strong cooling conditions.

The current from each cell was recorded, but not used, and showed unequal current distributions caused by the presence of the aged cell, which could lead to accelerated degradation due to the higher transient local currents and temperature inhomogeneities. Therefore, it is crucial to quickly identify aged cells so they can be replaced to maximise overall pack lifetime and performance.

DTV is more suitable as a diagnosis method for real-world applications compared to other common methods such as slow rate cyclic voltammetry, electrochemical impedance spectroscopy and incremental capacity analysis. This is because the method only requires a single surface temperature per cell and voltage measurement which are normally already available in modern applications for monitoring safety and SOC respectively. It does not require additional hardware like EIS, accurate and constant current measurement like ICA, or very slow and specific load profiles like SRCV. The installation cost in most cases should be minimal if the correct sensors are already in place, and it should be possible to handle the simple computation within most existing battery management systems.

In this paper, the use of DTV and DHFV has been demonstrated in a pack condition under constant current charge and thermal management which means the diagnosis can be carried whenever a smartphone or an electric vehicle is left to charge. In future work we will investigate how this novel thermal diagnosis technique can be used to extend battery pack lifetime and/or increase performance by combining it with adaptive control strategies. The work therefore represents a significant step forward in the transition to electric vehicles and promoting clean, sustainable transport.

Acknowledgement

The authors would also like to acknowledge Climate KIC for funding this work for Yu Merla as well as the EPSRC through the Career Acceleration Fellowship for Gregory Offer (EP/I00422X/1) and Low Carbon Grids Project (EP/K002252/1) for Billy Wu, the ESRN Energy Storage Research Network project for Vladimir Yufit and the FUTURE vehicles project (EP/I038586/1).

Appendix A. Supplementary data

Supplementary data related to this article can be found at http://dx.doi.org/10.1016/j.jpowsour.2016.09.008.

References

[1] G.J. Offer, D. Howey, M. Contestabile, R. Clague, N.P. Brandon, Comparative analysis of battery electric, hydrogen fuel cell and hybrid vehicles in a future sustainable road transport system, Energy Policy 38 (2010) 24–29, http://dx.doi.org/10.1016/j.enpol.2009.08.040.
[2] G.J. Offer, D. Howey, M. Contestabile, R. Clague, N.P. Brandon, Techno-economic and behavioural analysis of battery electric, hydrogen fuel cell and hybrid vehicles in a future sustainable road transport system in the UK, Energy Policy 39 (2011) 1939–1950, http://dx.doi.org/10.1016/j.enpol.2011.01.006.
[3] K. Bullis, How Tesla is driving electric car innovation, MIT Technol. Rev. (2013). http://www.technologyreview.com/news/516961/how-tesla-is-driving-electric-car-innovation/ (accessed 17.12.15).
[4] J. Vetter, P. Novák, M.R. Wagner, C. Veit, K.-C. Möller, J.O. Besenhard, et al., Ageing mechanisms in lithium-ion batteries, J. Power Sources 147 (2005) 269–281, http://dx.doi.org/10.1016/j.jpowsour.2005.01.006.
[5] S. Krueger, R. Kloepsch, J. Li, S. Nowak, S. Passerini, M. Winter, How do reactions at the anode/electrolyte interface determine the cathode performance in lithium-ion batteries? J. Electrochem. Soc. 160 (2013) A542–A548, http://dx.doi.org/10.1149/2.022304jes.
[6] G.J. Offer, V. Yufit, D.A. Howey, B. Wu, N.P. Brandon, Module design and fault diagnosis in electric vehicle batteries, J. Power Sources 206 (2012) 383–392, http://dx.doi.org/10.1016/j.jpowsour.2012.01.087.
[7] D. Andre, M. Meiler, K. Steiner, H. Walz, T. Soczka-guth, D.U. Sauer, Characterization of high-power lithium-ion batteries by electrochemical impedance spectroscopy. II: modelling, J. Power Sources 196 (2011) 5349–5356, http://dx.doi.org/10.1016/j.jpowsour.2010.07.071.
[8] I. Buchberger, S. Seidlmayer, A. Pokharel, M. Piana, J. Hattendorff, P. Kudejova, et al., Aging analysis of graphite/LiNi1/3Mn1/3Co1/3O2 cells using XRD, PGAA, and AC impedance, J. Electrochem. Soc. 162 (2015) A2737–A2746, http://dx.doi.org/10.1149/2.0711514jes.
[9] l. A. Huff, J.L. Rapp, L. Zhu, A.A. Gewirth, Identifying lithium-air battery discharge products through 6Li solid-state MAS and 1H-13C solution NMR spectroscopy, J. Power Sources 235 (2013) 87–94, http://dx.doi.org/10.1016/j.jpowsour.2013.01.158.
[10] F. Tariq, V. Yufit, D.S. Eastwood, Y. Merla, M. Biton, B. Wu, et al., In-operando X-ray tomography study of lithiation induced delamination of Si based anodes for lithium-ion batteries, ECS Electrochem. Lett. 3 (2014) A76–A78, http://dx.doi.org/10.1149/2.0081407eel.
[11] M. Ebner, F. Marone, M. Stampanoni, V. Wood, Visualization and quantification of electrochemical and mechanical degradation in Li ion batteries, Science 342 (2013) 716–720, http://dx.doi.org/10.1126/science.1241882.
[12] C. Hu, B.D. Youn, J. Chung, A multiscale framework with extended Kalman filter for lithium-ion battery SOC and capacity estimation, Appl. Energy 92 (2012) 694–704, http://dx.doi.org/10.1016/j.apenergy.2011.08.002.
[13] S. Lee, J. Lee, A Comparative Analysis of Techniques for Electric Vehicle Battery Prognostics and Health Management (PHM), 2016, http://dx.doi.org/10.4271/2011-01-2247.
[14] K. Maher, R. Yazami, A study of lithium ion batteries cycle aging by thermodynamics techniques, J. Power Sources 247 (2014) 527–533, http://dx.doi.org/10.1016/j.jpowsour.2013.08.053.
[15] M. Dubarry, C. Truchot, B.Y. Liaw, Cell degradation in commercial LiFePO4 cells with high-power and high-energy designs, J. Power Sources 258 (2014) 408–419, http://dx.doi.org/10.1016/j.jpowsour.2014.02.052.
[16] B. Wu, V. Yufit, Y. Merla, R.F. Martinez-botas, N.P. Brandon, G.J. Offer, Differential thermal voltammetry for tracking of degradation in lithium-ion batteries, J. Power Sources 273 (2015) 495–501, http://dx.doi.org/10.1016/j.jpowsour.2014.09.127.
[17] Y. Merla, B. Wu, V. Yufit, R.F. Martinez-botas, N.P. Brandon, G.J. Offer, Novel application of differential thermal voltammetry as an in-depth state of health diagnosis method for lithium-ion batteries, J. Power Sources 307 (2016) 308–319, http://dx.doi.org/10.1016/j.jpowsour.2015.12.122.
[18] B. Wu, V. Yufit, M. Marinescu, G.J. Offer, R.F. Martinez-Botas, N.P. Brandon, Coupled thermal–electrochemical modelling of uneven heat generation in lithium-ion battery packs, J. Power Sources 243 (2013) 544–554, http://dx.doi.org/10.1016/j.jpowsour.2013.05.164.
[19] M. Dubarry, C. Truchot, M. Cugnet, B.Y. Liaw, K. Gering, S. Sazhin, et al., Evaluation of commercial lithium-ion cells based on composite positive electrode for plug-in hybrid electric vehicle applications. Part I: initial characterizations, J. Power Sources 196 (2011) 10328–10335, http://dx.doi.org/10.1016/j.jpowsour.2011.08.077.
[20] M. Berecibar, F. Devriendt, M. Dubarry, I. Villarreal, N. Omar, W. Verbeke, et al., Online state of health estimation on NMC cells based on predictive analytics, J. Power Sources 320 (2016) 239–250, http://dx.doi.org/10.1016/j.jpowsour.2016.04.109.
[21] I. Bloom, A.N. Jansen, D.P. Abraham, J. Knuth, S.A. Jones, V.S. Battaglia, et al., Differential voltage analyses of high-power, lithium-ion cells 1. Technique and application, J. Power Sources 139 (2005) 295–303, http://dx.doi.org/10.1016/j.jpowsour.2004.07.021.
[22] T.C. O'Haver, peakfit.m, (n.d.). https://terpconnect.umd.edu/~toh/spectrum/peakfit.m (accessed 06.05.15).

[23] M. Dubarry, C. Truchot, B.Y. Liaw, Synthesize battery degradation modes via a diagnostic and prognostic model, J. Power Sources 219 (2012) 204–216, http://dx.doi.org/10.1016/j.jpowsour.2012.07.016.
[24] W.S. Yoon, K.Y. Chung, J. McBreen, X.Q. Yang, A comparative study on structural changes of LiCo1/3Ni1/3Mn1/3O2 and LiNi0.8Co0.15Al0.05O2 during first charge using in situ XRD, Electrochem. Commun. 8 (2006) 1257–1262, http://dx.doi.org/10.1016/j.elecom.2006.06.005.
[25] K.-W. Nam, W.-S. Yoon, H. Shin, K.Y. Chung, S. Choi, X.-Q. Yang, In situ X-ray diffraction studies of mixed LiMn2O4–LiNi1/3Co1/3Mn1/3O2 composite cathode in Li-ion cells during charge–discharge cycling, J. Power Sources 192 (2009) 652–659, http://dx.doi.org/10.1016/j.jpowsour.2009.02.088.
[26] N. Yabuuchi, Y. Makimura, T. Ohzuku, Solid-state chemistry and electrochemistry of LiCo[sub 1/3]Ni[sub 1/3]Mn[sub 1/3]O[sub 2] for advanced lithium-ion batteries, J. Electrochem. Soc. 154 (2007), http://dx.doi.org/10.1149/1.2455585. A314.
[27] M.D. Levi, D. Aurbach, The mechanism of lithium intercalation in graphite film electrodes in aprotic media. Part 1. High resolution slow scan rate cyclic voltammetric studies and modeling, J. Electroanal. Chem. 421 (1997) 79–88, http://dx.doi.org/10.1016/S0022-0728(96)04832-2.
[28] A. Papazoglou, S. Longo, D. Auger, F. Assadian, Nonlinear filtering techniques comparison for battery state estimation, J. Sustain. Dev. Energy, Water Environ. Syst. 2 (2014) 259–269, http://dx.doi.org/10.13044/j.sdewes.2014.02.0021.
[29] S.M. Rezvanizaniani, Z. Liu, Y. Chen, J. Lee, Review and recent advances in battery health monitoring and prognostics technologies for electric vehicle (EV) safety and mobility, J. Power Sources 256 (2014) 110–124, http://dx.doi.org/10.1016/j.jpowsour.2014.01.085.
[30] R.R. Richardson, P.T. Ireland, D.A. Howey, Battery internal temperature estimation by combined impedance and surface temperature measurement, J. Power Sources 265 (2014) 254–261, http://dx.doi.org/10.1016/j.jpowsour.2014.04.129.
[31] D.P. Abraham, E.M. Reynolds, P.L. Schultz, A.N. Jansen, D.W. Dees, Temperature dependence of capacity and impedance data from fresh and aged high-power lithium-ion cells, J. Electrochem. Soc. 153 (2006) A1610, http://dx.doi.org/10.1149/1.2210668.
[32] J.B. Robinson, J.A. Darr, D.S. Eastwood, G. Hinds, P.D. Lee, P.R. Shearing, et al., Non-uniform temperature distribution in Li-ion batteries during discharge - a combined thermal imaging, X-ray micro-tomography and electrochemical impedance approach, J. Power Sources 252 (2014) 51–57, http://dx.doi.org/10.1016/j.jpowsour.2013.11.059.
[33] E. Arabmakki, M. Kantardzic, T.S. Sethi, RLS-A Reduced Labeled Samples Approach for Streaming Imbalanced Data with Concept Drift, 2014, pp. 779–786.